

RESEARCH

Open Access



Pericyte-derived extracellular vesicles improve vascular barrier function in sepsis via the Angpt1/PI3K/AKT pathway and pericyte recruitment: an in vivo and in vitro study

Zi-sen Zhang^{1†}, Ao Yang^{1†}, Xi Luo^{2†}, He-nan Zhou¹, Yi-yan Liu¹, Dai-qin Bao², Jie Zhang¹, Jia-tao Zang¹, Qing-hui Li¹, Tao Li^{1**†} and Liang-ming Liu^{1**†}

Abstract

Background Extracellular vesicles derived from pericytes (PCEVs) have been shown to improve vascular permeability, with their therapeutic effects attributed to the presence of pro-regenerative molecules. We hypothesized that angiopoietin 1 (Angpt1) carried by PCEVs contributes to their therapeutic effects after sepsis.

Methods A cecal ligation and puncture (CLP)-induced sepsis rat model was used in vivo, and the effects of PCEVs on vascular endothelial cells were studied in vitro. First, proteomic and Gene Ontology enrichment analyses were performed to analyze the therapeutic mechanism of PCEVs, revealing that the angiogenesis-related protein Angpt1 was highly expressed in PCEVs. We then down-regulated Angpt1 in PCEVs. The role of PCEV-carried Angpt1 on intestinal barrier function, PCs recruitment, and inflammatory cytokines was measured by using septic Sprague–Dawley rats and platelet-derived growth factor receptor beta (PDGFR-β)-Cre + mT/mG transgenic mice.

Results PCEVs significantly improved vascular permeability, proliferation, and angiogenesis in CLP-induced gut barrier injury both in vivo and in vitro. Further studies have shown that PCEVs exert a protective effect on intestinal barrier function and PC recruitment. Additionally, PCEVs reduced serum inflammatory factor levels. Our data also demonstrated that the protein levels of phospho-PI3K and phospho-Akt both increased after PCEVs administration, whereas knocking out Angpt1 suppressed the protective effects of PCEVs through decreased activation of PI3K/Akt signaling.

Conclusion PCEVs protect against sepsis by regulating the vascular endothelial barrier, promoting PC recruitment, protecting intestinal function, and restoring properties via activation of the Angpt1/PI3K/AKT pathway.

Keywords Sepsis, Pericytes, Extracellular vesicles, Angpt1, Vascular barrier function

[†]Tao Li and Liangming Liu have contributed equally to this work.

[†]Zi-sen Zhang, Ao Yang and Xi Luo have contributed as co first authors.

*Correspondence:

Tao Li

lt200132@tmmu.edu.cn

Liang-ming Liu

lmliu62@tmmu.edu.cn

Full list of author information is available at the end of the article



Background

Sepsis is a severe medical illness marked by a dysregulated systemic inflammatory response to infection, considerably impacting global death rates. This complex condition can cause deterioration of multiple inflammatory, leading to multi-organ dysfunction syndrome (MODS) [1]. A key factor in the progression of MODS during sepsis is the hyperpermeability of vascular endothelial cells (VECs) [2, 3]. Thus, restoring endothelial barrier integrity is essential for maintaining vascular homeostasis and tissue-fluid balance in treating severe sepsis and related multiple-organ dysfunction.

Pericytes (PCs) are pluripotent cells that regulate the microenvironment by irrigation flow and permeability. Previous studies have demonstrated that PCs are involved in various diseases such as diabetes, hypertension, diabetic retinopathy, cardiovascular disease, inflammation, trauma, Alzheimer's disease, multiple sclerosis, and tumor formation [4]. Recent studies showed that the secretome of PCs, which includes platelet-derived growth factor receptor beta (PDGFR- β), angiopoietins-1 (Angpt1), vascular endothelial growth factor (VEGF), and transforming growth factor- β (TGF- β), has potential implications for tissue regeneration [5].

Recently, emerging evidence suggests that cell-derived extracellular vesicles (EVs) transfer bioactive molecules to regulate the development of various inflammatory diseases [6, 7]. Our previous study found that PCs could deliver EVs containing TGF- β and microRNAs, which are involved in regulating vascular barrier functions after sepsis [8, 9], and other studies have shown that Angpt1 derived from PCs protects VECs against brain and lung injuries [10, 11]. Angpt1 acts as a Tie 2 agonist, triggering endothelial cell survival, permeability, and proliferation possibly by activating the phosphatidylinositol 3-kinase (PI3K)/Akt signaling pathway [12]. Angpt1 in endothelial cells (ECs) also recruits PCs and promotes PC coverage, enhancing vascular endothelial integrity [13]. However, it is unclear whether EVs derived from PCs have therapeutic effects on gut barrier function after sepsis. Additionally, the role of EVs derived from pericytes (PCEVs) in sepsis and related mechanisms remains unexplored. Therefore, this study aimed to fill this gap by investigating the therapeutic effects of PCEVs on vascular and intestinal barrier functions in sepsis and determining whether Angpt1 plays a key role in mediating these protective effects through the PI3K/Akt signaling pathway.

Materials and methods

In vivo assay

Animals

All animal experiments were approved by the Laboratory Animal Welfare and Ethics Committee of Third

Military (Army) Medical University (approval no. AMUWEC20210873). Adult healthy Sprague–Dawley (SD) rats were obtained from the Animal Center of the Research Institute of Surgery at the Army Medical University (Chongqing, China). PC fluorescent-labeled mice (PDGFR- β -Cre + mT/mG transgenic mice) were successfully constructed in our laboratory [8]. The animals were housed in a controlled environment with a temperature of 22 ± 2 °C, relative humidity between 40 and 60%, and a 12-h cycle of light and darkness with free access to food and drink. Forty-four rats and 18 PDGFR- β -Cre + mT/mG transgenic mice were used in this study. The reporting of animal experiments for this study adhered to the ARRIVE guidelines 2.0.

Preparation of septic shock model in rats and mice

Thirty-six SD rats and 15 PC transgenic mice (8–12 w of both sexes) were anesthetized with by intraperitoneal injection of 45 mg/kg sodium pentobarbital and kept under anesthesia during the entire surgical procedures. The sepsis model was induced by cecal ligation and puncture (CLP) [14]. Briefly, a laparotomy was performed, the cecum was exposed and ligated, and two holes were punctured 1 cm from the distal end using a triangular needle (approximately 1.5 mm in diameter). Feces were allowed to flow into the abdominal cavity. After abdominal closure, the rats and mice were returned to their cages and allowed ad libitum access to food and water. A septic shock model was considered successful 12 h post-surgery if the mean arterial pressure was less than 70 mmHg. The success rate of septic shock in this study was approximately 89% out of the thirty-two rats and 12 PC transgenic mice that were initially enrolled. The unsuccessful animal models were euthanized with excessive pentobarbital sodium (100 mg/kg, intraperitoneally).

The experimental design

Rats and PC transgenic mice were randomized into the following groups: 1) sham group: a group without CLP and treatment, undergoing an operation similar to the other groups ($n = 8$ rats, $n = 3$ mice); 2) septic shock group ($n = 8$ rats, $n = 3$ mice); 3) PCEVs group ($n = 8$ rats, $n = 3$ mice); 4) Angpt1 siRNA PCEVs group ($n = 8$ rats, $n = 3$ mice); and 5) negative siRNA PCEVs group ($n = 8$ rats, $n = 3$ mice). The PCEV dose was based on prior studies [9]. Consequently, we administered 200 μ L of PCEVs. Tail vein injection was performed for the different groups at 12 h after CLP establishment. After 24 h and in separate experiments, the dynamics of FITC-BSA leakage and green-expressing PCs from the mesenteric microvessels in rats and PC transgenic mice were measured by intravital microscopy. Before dissection, rats were euthanized with excessive pentobarbital sodium. The retinal and

mesenteric veins and mesenteric arteries from sham rats were collected for cell culture. Mesenteric microvessels, the small intestine, and blood were collected from rats for assessing levels of histological, protein, and inflammatory markers (Fig. 1).

Measurement of vascular leakage and blood flow velocity in mesenteric microvessels in vivo

Vascular leakage

Albumin leakage across the mesenteric venular wall was evaluated using a high-speed video camera system (C11440, Hamamatsu, Shizuoka, Japan) with fluorescein isothiocyanate-bovine serum albumin (FITC-BSA). After anesthesia administration, the rat's abdomen was accessed by making a 2–3 cm midline incision. A section of the mesentery, known as the ileocecal segment, measuring 10–15 cm, was brought outside the body and placed on a clear plastic platform. The mesentery was maintained at a constant temperature of 37 °C and kept moist with continuous superfusion using saline solution. The mice received an intravenous injection of FITC-BSA (50 mg/kg). Following 10 min of baseline observation, an intravenous injection of 50 mg/kg FITC-BSA was administered, and images were recorded at 0, 1, 3, and 6 min, after which the fluorescence intensity of FITC-BSA was measured. The area of FITC-BSA⁺ per vessel was quantified.

Mesenteric blood flow velocity

Arterioles and venules without obvious bend and with diameters ranging from 30 to 50 μm were used to measure blood flow velocity. The velocity of red blood cells in the microvessel was measured using a high-speed video camera system at a rate of 1000 frames per second (fps)

and analyzed using the ImageJ software (v1.8.0). The captured images were replayed at 5 fps.

Harvesting and immunohistochemistry of rat mesentery tissue

Rat mesenteric microvessels were collected for immunohistochemical analysis under each experimental condition. Mesenteric tissues were collected from the gut using sterile techniques with microscissors and forceps. Prior to collection, the tissues were exposed to 4% phosphate-buffered paraformaldehyde for 25 min followed by fixation with 4% paraformaldehyde at 4 °C overnight. Subsequently, the samples were thoroughly rinsed with PBS and then incubated at 37 °C for 30 min in a solution containing 0.1% Triton X-100 in PBS. Following three rinses with 0.1 M PBS, the samples were incubated with a blocking solution that included 5% BSA. Next, PBS was used to clean the samples, and VE-cadherin (555,289, BD Biosciences, Franklin Lakes, NJ, USA) and ZO-1 antibodies (33–9100, Invitrogen, Waltham, MA, USA) were used to label them.

Ultrastructure of the tight junction and microvilli in mesenteric microvessels and small intestine

Rat mesenteric microvessels and small intestines were collected for electron microscopy analysis under each experimental condition. The mesentery was first exposed to a 3% glutaraldehyde solution in 0.1 M PBS for 20 min. Following this, the mesentery was divided into blocks smaller than 1 mm³ and further fixed by immersing them in the same fixative for 1 h at room temperature (RT), followed by overnight incubation at 4 °C. Following rinsing, the tissues underwent post-fixation using a solution containing 1% osmium tetroxide in 0.1 M PBS for 2 h at a temperature of 4 °C. Subsequently, the tissues were dried

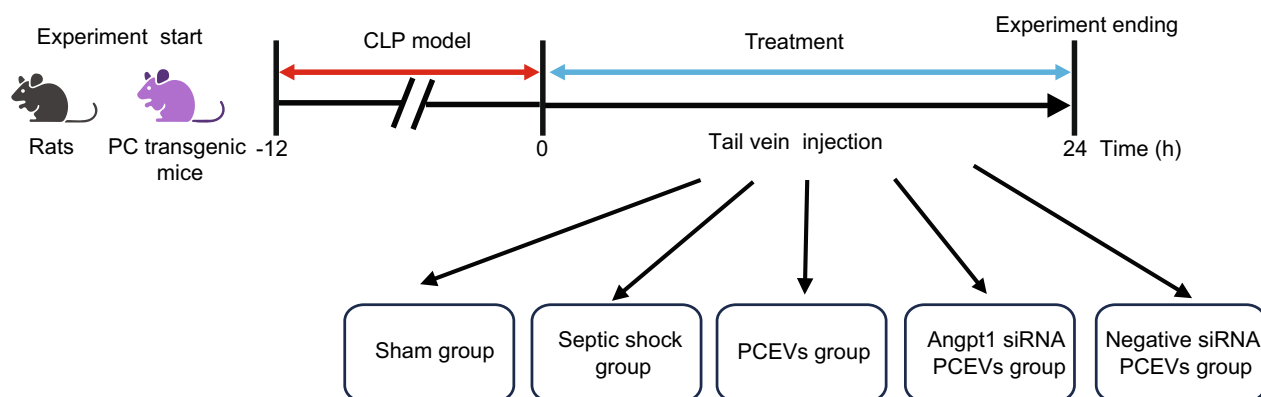


Fig. 1 A schematic demonstrating the experimental design. The rats and mice were divided into five groups: sham, septic shock, PCEVs, Angpt1 siRNA PCEVs, and negative siRNA PCEVs group, with eight rats and three mice in each group

and embedded in Epon 812 and ultrathin slices were stained with uranyl acetate and lead citrate and examined using transmission electron microscopy (TEM) (JEM 1400; JEOL, Tokyo, Japan). For routine histological examination, the length of the villi was measured.

Immunohistochemistry analyses

Following the sacrifice of the rats, 10 cm sections of each part of the digestive tract were carefully removed. These sections were then washed with ice-cold PBS and rolled into "Swiss rolls" [15]. The intestinal tissue was preserved by immersion in a 4% formaldehyde solution for 24 h at RT. Following fixation, the tissues were immersed in paraffin, sectioned into 4 μm slices, and mounted onto slides. The tissue slides were deparaffinized, rehydrated, and subjected to hematoxylin and eosin staining. The severity of pathological injury was evaluated using the scoring system (Chiu's score). Grade 0 represented normal villi, while grades 1–5 indicated increments in injury severity [16].

Assessment of the blood flow in the intestines

Intestinal blood flow was measured using Doppler imaging (Peri Cam PSI ZR, Sweden). The organ was subjected to a laser at a distance of 14 cm and intestinal blood flow was assessed using the PIM software.

In vitro assay

PCs and isolation of PCEVs

Retinal microvascular pericytes (RMPs) were isolated from rats and cultured in a PC medium (PCM; Cat. no.1201, ScienCell, Carlsbad, CA, USA) [17]. Cells were labeled using antibodies specific to the following markers: platelet-derived growth factor receptor- β (PDGFR- β ; ab32570, Abcam, Cambridge, UK), nerve/glia antigen 2 (NG2; ab5320, Merck Millipore, Burlington, MA, USA), CD146 (ab75769, Abcam), α -smooth muscle actin (α -SMA; ab7817, Abcam), and platelet endothelial cell adhesion molecule (CD31; ab24590, Abcam). Flow cytometry was performed by labeling cells with directly conjugated antibodies, namely NG-2-APC, PDGFR- β -APC, CD146-PE, CD31-PE, IgG-APC, and IgG-PE, all obtained from BD Biosciences. Samples were analyzed using a high-sensitivity imaging flow cytometer (Amnis ImageStream MK II; ISX).

PCEVs were isolated from the cell supernatant after 48 h in a fresh conditioned medium (PCM without FBS) through successive centrifugations [18]. In summary, the cell medium was centrifuged at 1,500 g for 5 min, resulting in the collection of a cell debris-free supernatant. The liquid portion was centrifuged at 16,000 \times acceleration due to gravity for 1 h. The EVs were then subjected to three washes with 1 mL of phosphate-buffered saline

(PBS) at a centrifugal force of 16,000 g for 45 min. Subsequently, the pellet containing EVs was resuspended in PBS at 10 μL PCEVs per 1×10^6 cells and then kept at -80°C for future experiments.

Preparation of vascular smooth muscle cells (VSMCs) and VECs

VSMCs and VECs were isolated from the mesenteric arteries and veins of SD rats by enzymatic digestion [8] and then cultured in a smooth muscle cell medium (SMCM; Cat. No.1101, ScienCell) and an endothelial cell medium (Cat. No.1001, ScienCell), respectively. Before each experiment, VSMCs and VECs (passages 3–5) were serum-starved for 24 h.

TEM of PCEVs

TEM was performed using negative staining and ultrathin slices. The measurement of EV preparations for negative staining was conducted as previously described [21]. Pelleted EVs were treated with a solution of 2.5% glutaraldehyde in PBS at 4°C for 24 h to prepare ultrathin sections. After rinsing with 0.1 M PBS twice, the samples were further treated with 1% OsO₄ at RT for 70 min to complete the fixation process. Following three rinses with 0.1 M PBS, samples were dehydrated with ethanol at increasing concentrations. Finally, the samples were immersed in Epon 812 and thin slices measuring 100 nm were created on the grids. The EVs were examined by TEM using a JEM 1400 instrument (JEOL Instruments).

PCEVs with or without Angpt1 siRNA adenovirus transfection

PCs employed to evaluate the optimal multiplicity of infection (MOI) were seeded onto a six-well plate at 1×10^5 cells/well and cultured in PCM for 24 h before adenovirus infection (Obio Biomedical Technology, Shanghai, China). LacZ adenovirus (Obio) was used as a negative control. The adenoviral vectors were diluted to three gradients of 5×10^8 , 5×10^7 , and 5×10^6 PFU/mL. The medium was replaced after 6 h and infectivity was determined by observing green fluorescent protein expression after 48 h under an inverted fluorescence microscope (DMI3000B, Leica, Wetzlar, Germany). An MOI of 5×10^7 provided the best transfection efficiency (Supplemental Fig. 1a).

Enzyme-linked immunosorbent assay (ELISA)

ELISAs from PCs and PCEVs were performed using Quantikine ELISA Kits for VEGF (ab100786, Abcam), Angpt1 (ab213920, Abcam), and TGF- β 1 (ab119558, Abcam) according to the manufacturer's instructions. Blood was centrifuged to measure levels of IL-6 (ab242739, Abcam), IL-1 β (ab255730, Abcam), and

TNF- α (ab236712, Abcam) using ELISA kits according to the manufacturer's instructions.

Co-culture of LPS-stimulated VECs and PCEVs

VECs were placed on inserts of a six-cell culture plate with a pore size of 0.4 μm (product code 3450; Corning, Corning, NY, USA). VECs were exposed to lipopolysaccharide (LPS, *Escherichia coli* serotype O111:B4, Sigma-Aldrich, St. Louis, MO, USA) stimulation at 1 $\mu\text{g}/\text{mL}$ for 12 h and then co-cultured with Angpt1 siRNA PCEVs, negative siRNA PCEVs, and PCEVs (30 μL), respectively. The transendothelial electrical resistance (TER) of ECs was evaluated using a Voltohmmetre (World Precision Instruments Inc., Sarasota, FL, USA) at 30-min intervals for 24 h. After completing the TER study, the penetration rate was determined. Inserts were then treated with FITC-BSA, and 200 μL of the resulting liquid was collected every 10 min. At the same time, 200 μL of new basal media was added. The penetration rate was determined by dividing the total supernatant fluorescence OD by the FITC-BSA-stained fluorescence OD [9, 22]. Immunofluorescence and western blotting were used to identify the presence of ZO-1 and VE-cadherin in VECs after 24 h in independent experiments.

Sample preparation and mass spectrometry

Proteomic analysis was conducted by Shanghai Applied Protein Technology Co., Ltd. (Shanghai, China). PCEVs were collected according to the specified method (PC-EV1, PC-EV2, and PC-EV3), whereas smooth muscle cell-derived extracellular vesicles (SEVs) were used as the control group (SMC-EV1, SMC-EV2, and SMC-EV3). The EV samples were examined at an Applied Protein Technology Biolaboratory in China using a Q Exactive mass spectrometer (Thermo Fisher Scientific, Waltham, MA, USA). The samples were mixed with SDT buffer A (4% SDS, 100 mM Tris-HCl, 1 mM DTT, pH 7.6) and quantified using the BCA method (Bio-Rad Laboratories, Hercules, CA, USA). DTT and detergent were then removed from the solution by ultrafiltration (using Microcon units with a molecular weight cutoff of 10 kDa) and UA buffer (8 M urea, 150 mM Tris-HCl, and pH 8.0). Samples were then supplemented with 100 μL of iodoacetamide (100 mM IAA in UA buffer) and incubated in the dark for 30 min. Protein suspensions were then digested overnight using 4 μg of trypsin in a 25 mM NH_4HCO_3 buffer at RT of 37 $^\circ\text{C}$. The digested peptides were collected using a filter desalinated using a C18 (Sigma-Aldrich), concentrated by vacuum centrifugation, and reconstituted in 0.1% formic acid.

LC-MS/MS was conducted using a Q Exactive mass spectrometer (Thermo Fisher Scientific) connected to an Easy nLC (Proxeon Biosystems, now Thermo Fisher

Scientific) for 120 min. Purified peptides were introduced into a reverse-phase trap column (Thermo Fisher Scientific) and connected to a C18-reversed phase analytical column (Thermo Fisher Scientific) using 0.1% formic acid buffer A. Samples were separated using gradient buffer B (0.1% formic acid and 84% acetonitrile) at a flow rate of 300 nL/min. The purified peptides were analyzed using mass spectrometry. Data were gathered using a data-dependent approach that dynamically selects precursor ions from a scan range of 300–1800 m/z. The following settings were applied: an automated gain control goal set at $3e^6$, a maximum injection time of 10 ms, a dynamic exclusion length of 40 s, a survey scan resolution of 70,000 at m/z=200, an isolation width of 2 m/z, and a normalized collision energy of 30 eV. The peptide-recognition mode was activated during operation [21].

Data acquisition and DEG functional enrichment analysis

The MS data were analyzed and processed using the MaxQuant software (v1.5.3.09) for identification and quantitation. The False Discovery Rate was established at ≤ 0.01 . Peptides were selected for quantification based on the criteria for the use of razors and distinct peptides. Protein abundance was determined using normalized spectral protein intensity, also known as the label-free quantification intensity. Differentially expressed genes (DEGs) were identified using microarray data for PC proteomics obtained from the Gene Expression Omnibus database (<https://www.ncbi.nlm.nih.gov/geo/>) using the accession codes GSE195917 and GSE190809. Statistical significance was assessed using Student's t-test, with a threshold of $P < 0.05$. Significant differences were indicated by a ratio of ≥ 2 or ≤ 0.5 .

A Gene Ontology (GO) study was conducted using the DAVID online database to examine the functions of DEGs. The functional validity of the DEGs was confirmed using the FunRich platform, which examined the cellular components, molecular functions, biological processes, and biological pathways of these DEGs. A P value of less than 0.05 was considered statistically significant.

Angiogenesis measurement

The Matrigel Matrix (Corning) was thawed at 4 $^\circ\text{C}$ and carefully applied to the μ -slides (ibidi). The μ -slides were then incubated at 37 $^\circ\text{C}$ for 1 h. Subsequently, VECs were placed over the matrix and exposed to LPS and PCEV according to the experimental protocol. The μ -slides were examined using Leica SP5 laser confocal microscopy (Leica) [22]. The tubes and junctions of the angiogenesis analysis were quantified using the ImageJ software (v1.8.0).

Migration of VECs

The migration of VECs was assessed using a six-well plate (Corning). The VECs were introduced at a concentration of 1×10^5 cells/well and allowed to grow until they covered the entire cell surface. The medium was then replaced with DMEM-F12, and a sterile pipette was used to create a straight line at the center of the well. Subsequently, the vascular VECs were cleansed, cultivated with various interventions, and examined using a microscope (Leica) at both 0 and 24 h. The width of migration was determined using the ImageJ software. The migration ratio was calculated as follows: [width (at 0 h) - width (at 24 h)] / width (at 0 h).

CCK8 analysis

VECs were cultured in a 96-well plate (Corning) at 1×10^3 cells/well seeding density. When the cells reached 75% confluence, the medium was replaced with 100 μ L of serum-free medium. Subsequently, 10 μ L of CCK8 detection solution (HY-K0301, MCE) was added to each well, and the plate was incubated at 37 °C for 1.5 h. Absorbance was measured at 450 nm using a Microplate Reader (Thermo Fisher Scientific). The CCK8 value was determined using the following formula: (A_{sample} × A_{blank}) / (A_{control} × A_{blank}).

Western blot analysis

Western blot analysis was performed to assess the expression of ZO-1, VE-cadherin, Angpt1, Tie-2, p-Tie2, Akt, p-Akt, NF- κ B/p65, and p-NF- κ B/p65 using specific antibodies against ZO-1 (1:1000), VE-cadherin (1:1000), Angpt1 (1:2000; ab183701, Abcam), Tie-2 (1:2000; ab221154, Abcam), p-Tie2 (1:2000; ab151704, Abcam), PI3K (1:2000; ab40776, Abcam), p-PI3K (1:2000; ab138364, Abcam), AKT (1:2000; 9272, Cell Signaling Technology, Danvers, MA, USA), p-AKT (1:2000; 9271S, Cell Signaling Technology), NF- κ B/p65 (1:2000; 8242S, Cell Signaling Technology), p-NF- κ B/p65 (1:2000; 3033S, Cell Signaling Technology), and β -actin (1:7000; 4767S, Cell Signaling Technology) respectively. Bands were detected using fluorescent secondary antibodies and quantified using an Odyssey CLx Infrared Imaging System (LI-COR, Lincoln, NE, USA).

Statistical analysis

Data were presented as mean \pm SD. Differences among several groups were analyzed using ANOVA. All statistical analyses were conducted using the SPSS software (version 11.0) and GraphPad Prism software (San Diego, CA, USA). A value of $p < 0.05$ was considered statistically significant, where N in the figure legends refers to the number of participants (samples or rats).

Results

Isolation and characterization of PCEVs

As previously described, primary RMPs were successfully cultivated from rats [17]. PCs were characterized using immunohistochemistry. The staining for NG-2, PDGFR- β , CD146, and α -SMA of PC markers revealed that the cells in the culture showed positive immunofluorescence and flow cytometry. Importantly, no cells in the culture expressed positive staining for CD31, a specific marker for ECs (Fig. 2a and b).

EVs were isolated from the PCM of the RMPs. For all experiments, 10 μ L of PCEVs were collected from 10^6 serum-starved PCs over 48 h. The viability of these serum-starved PCs was >90% at 48 h before PCEVs isolation. Using TEM, PCEVs were measured in ultrathin sections (Fig. 2c) and with negative staining (Fig. 2d). Dynamic light scattering analysis indicated that the size of the PCEVs ranged from 100 to 1000 nm (Fig. 2e).

Detection of Angpt1 in PCEVs by proteomic analysis

Our previous study demonstrated that PCs can release EVs that play an important role in vascular barrier function after sepsis. Additionally, PCs can release angiogenic growth factors including Angpt1, TGF- β , and VEGF, which promote the development and stabilization of blood vessels. Thus, we first analyzed changes in the transcriptomic signature of vascular PCs from the GEO databases (GSE195917 and GSE190809). We analyzed DEGs (fold change > 1.5 and P value < 0.05) in PCs and SMCs using the GSE195917 and GSE190809 datasets. GO enrichment analysis showed these DEGs were involved in cell components, molecular function, and biological processes including regulating vascular permeability, endothelial cell proliferation, and angiogenesis (Fig. 3a

(See figure on next page.)

Fig. 2 Primary pericyte (PC) identification and electron microscopy images of extracellular vesicles derived from PCs (PCEVs). **a** PC immunofluorescence using confocal laser scanning microscopy (CLSM). PCs show positive immunostaining for NG-2, PDGFR- β , CD146, and α -SMA, whereas VECs show positive immunostaining for CD31. Scale bars: 100 μ m. **b** Characterization of PCs by flow cytometry. The gray histogram represents the isotype control. The black histogram shows the fluorescence intensity of PCs after incubation with NG-2, PDGFR- β , CD146, and CD31 antibodies. **c** Identification of PC-derived EVs by ultrathin sections. **d** Identification of PCEVs by negative staining. **e** PCEV diameter measured by DLS analysis

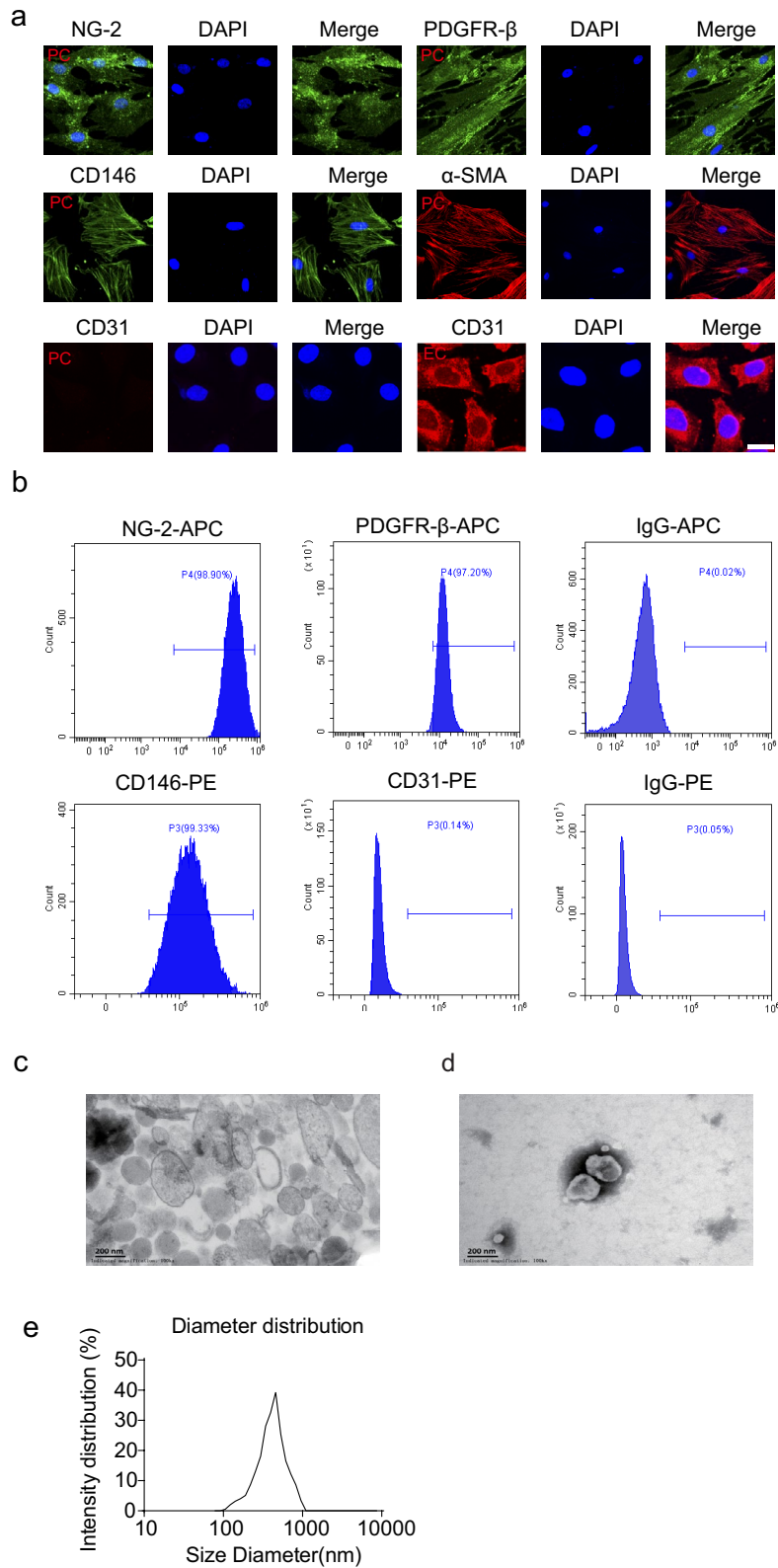


Fig. 2 (See legend on previous page.)

and b). Additionally, both datasets exhibited the expression of *Angpt1* in a heatmap linked to vascular function (Fig. 3c–d).

To investigate the presence of *Angpt1* in PCEV, we then conducted a proteomic analysis using mass spectrometry to determine the protein expression profiles of PCEVs and SEVs. We screened 280 differential upregulated genes and performed the GO enrichment analysis (Supplemental table). Pathway enrichment analysis further revealed that the most significantly altered pathways were involved with regulating vascular permeability and angiogenesis. The heatmap associated with vascular functions revealed significant *Angpt1* expression (Fig. 3e–f). Therefore, we examined *Angpt1* expression in PCEVs and SEVs. The findings showed that the expression of *Angpt1* was greater in PCEVs than in SEVs (Fig. 3g). In addition, we identified the growth factors associated with PCs such as *Angpt1*, VEGF, and TGF- β , which play a crucial role in paracrine signaling. PCs and PCEVs showed the highest *Angpt1* expression (Fig. 3h). These findings indicate that the presence of *Angpt1* in PCEV may significantly impact vascular endothelial barrier function.

PCEV-delivered *Angpt1* mediates protective effects on endothelial permeability of VECs in vitro

Co-incubation of PKH-26-labeled PCEVs and VECs showed that PCEVs were absorbed in a time-dependent manner (Fig. 4a). To examine the effect of *Angpt1* delivered by PCEVs on VEC function, we transfected PCs with *Angpt1* siRNA and isolated *Angpt1* siRNA PCEVs (Supplemental Fig1a). The results showed that the level of *Angpt1* was diminished by 82.9% in *Angpt1* siRNA transfected PCs compared with the negative siRNA group and remained downregulated by 62% in *Angpt1* siRNA PCEVs compared with negative siRNA PCEVs (Supplemental Fig1b).

After LPS stimulation for 12 h, 2×10^6 PCEVs were incubated with the VECs for 24 h to investigate the effects of PCEVs on VECs. Compared to LPS-stimulated VECs, the addition of PCEVs and negative siRNA PCEVs to LPS-stimulated VECs significantly improved TER and permeability to FITC-BSA. However, administration of *Angpt1* siRNA PCEV remarkably attenuated the PCEV-induced enhancement of vascular barrier function compared to the negative siRNA PCEV group (Fig. 4b and

c). Similarly, these results were corroborated by western blotting and immunohistochemistry results (Fig. 4d and e, Supplemental Fig. 2a).

PCEV-delivered *Angpt1* mediates protective effects on vascular endothelial barrier function after sepsis in vivo

To investigate the absorption of PCEVs by VECs *in vivo*, PKH-26-labeled PCEVs were infused intravenously into sepsis rats. The results showed a large amount of scattered red fluorescence in the mesenteric venule (Fig. 5a), indicating that PCEVs could be effectively absorbed by VECs. Compared to the septic shock group, PCEV administration significantly reduced albumin leakage. However, the addition of *Ang-1* siRNA PCEVs significantly increased albumin leakage compared with PCEVs (Fig. 5b). Similarly, PCEVs significantly improved the arteriolar and venular velocities in mesenteric microvessels, while *Angpt1* siRNA PCEVs attenuated the PCEV-induced improvement in blood flow velocity (Fig. 5c and supplemental Movies 1–5). Treatment with PCEVs increased the expression of ZO-1 and VE-cadherin in mesenteric microvessels, whereas *Angpt1* siRNA PCEVs attenuated the PCEV-induced improvement in vascular endothelial junctions (Fig. 5d and e, Supplemental Fig. 2b). Electron microscopy showed that PCEV treatment improved tight junction opening; however, this effect was attenuated by *Angpt1* siRNA PCEVs. These findings suggest that *Angpt1* siRNA PCEVs weakened the beneficial effects of PCEVs on vascular barrier function (Fig. 5f).

PCEV-delivered *Angpt1* mediates protective effects on endothelial proliferative and angiogenic functions of VECs in vitro

LPS stimulation significantly decreased the migration and proliferation abilities of VECs. However, PCEVs significantly increased these abilities, with growth rates of 52.5% and 37.4%, respectively. Conversely, *Angpt1* siRNA PCEV administration remarkably attenuated the PCEV-induced improvement in the migration and proliferation abilities of VECs (Fig. 6a and b). *Angpt1* is a well-known angiogenic growth factor. Therefore, we evaluated the angiogenic potential of *Angpt1* in LPS-stimulated PCEVs. We found that PCEVs significantly enhanced

(See figure on next page.)

Fig. 3 Identification of *Angpt1* in PCEVs by proteomic analysis and ELISA. **a, b** Gene ontology (GO) results of differentially expressed genes (DEGs) from the GSE195917 and GSE190809 datasets categorized into biological process (BP), cellular component (CC), and molecular function (MF). **c, d** Heatmap in vascular endothelial function pathways. **e, f** GO enrichment analysis of upregulated DEGs in PCEVs and heatmap in vascular endothelial function pathways. **g** Expression levels of *Angpt1* in PCs, SMCs, PCEVs, and SMCEVs as determined by ELISA ($n = 3$). **h** Quantification by multiplex sandwich ELISA of *Angpt1*, VEGF, and TGF- β 1 concentrations in PCs and PCEVs ($n = 3$). *** $P < 0.001$

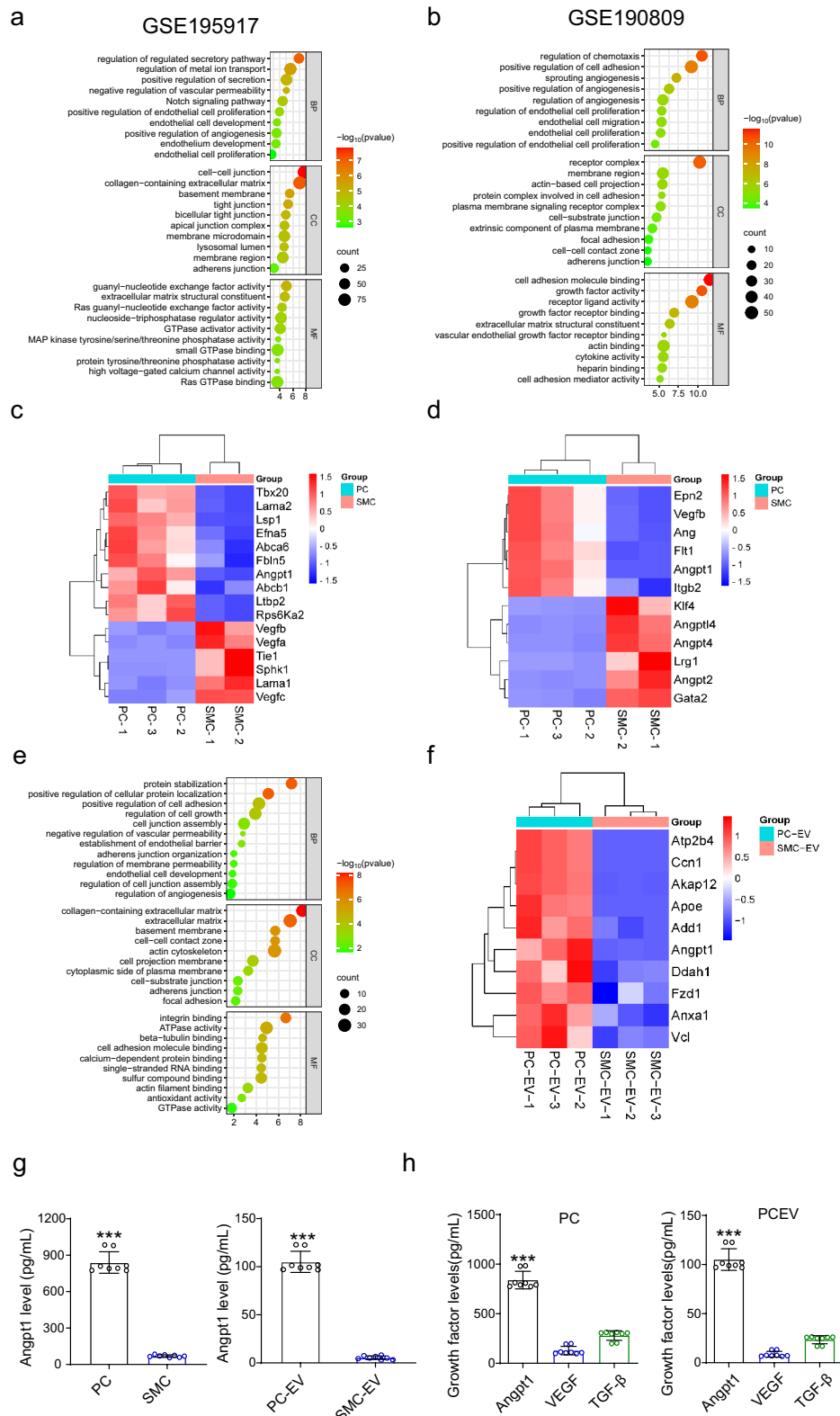


Fig. 3 (See legend on previous page.)

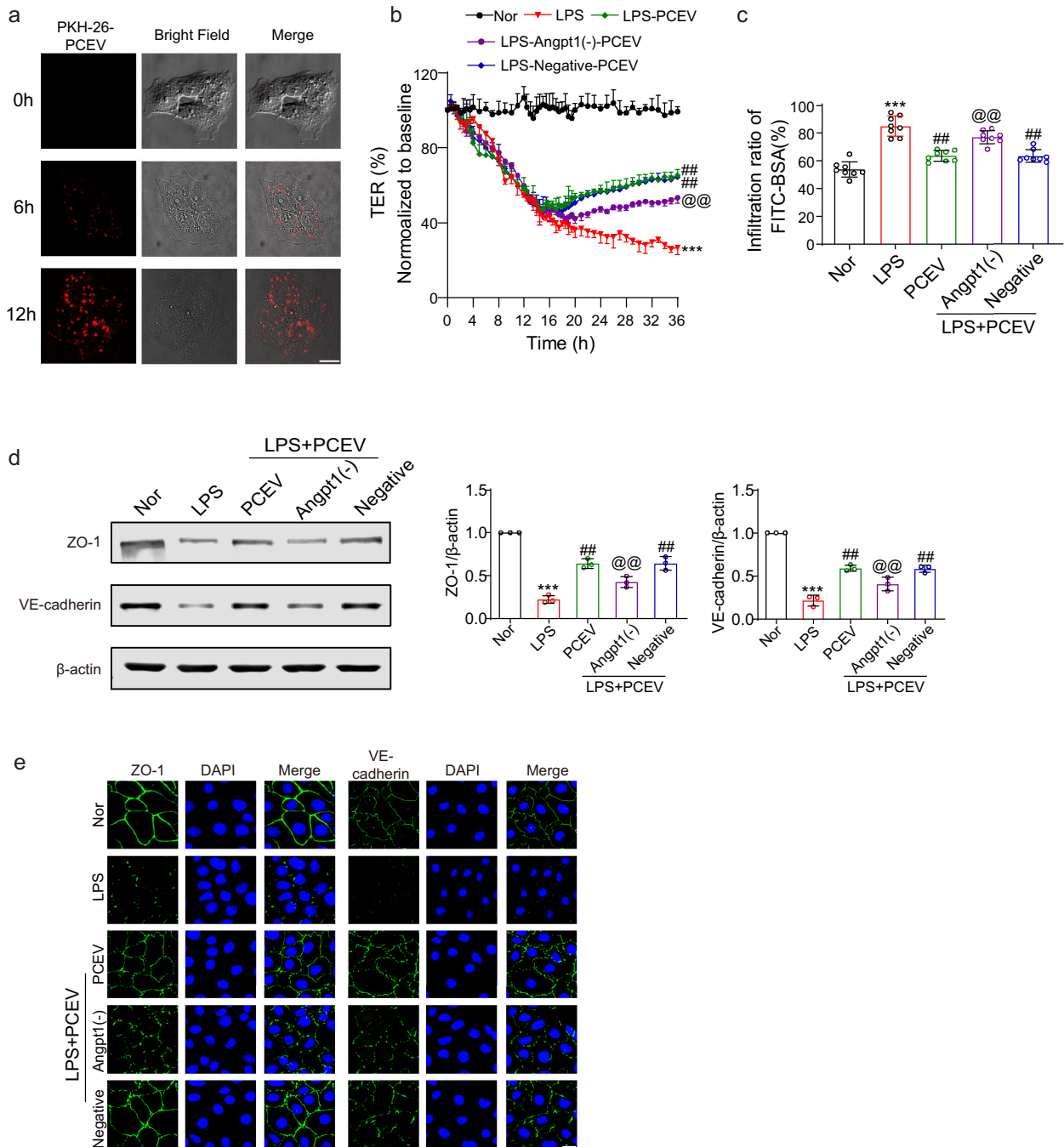


Fig. 4 Effects of Angpt1 carried by PCEVs on VEC barrier functions following LPS administration in vitro. **a** Illustrative images of the internalization of PKH-26-labeled PCEVs in VECs. Scale bars: 10 μ m. **b** PCEVs were added to VECs, and the TER of each group was measured (n=3). **c** PCEVs were added to VECs, and FITC-BSA penetration of each group was measured (n=8). **d** VECs treated with PCEVs were analyzed by western blotting (n=3). **e** VECs treated with PCEVs were analyzed by immunofluorescence for ZO-1 and VE-cadherin. Scale bars: 10 μ m. *** P <0.001 vs. Nor, ## P <0.01 vs. LPS, @@ P <0.01 vs. PCEV (one-way ANOVA)

tube formation parameters such as the number of nodes and junctions, whereas Angpt1 siRNA PCEVs inhibited their angiogenic functions (Fig. 6c).

PCEV-delivered Angpt1 mediated the PI3K/AKT pathway activity

The PI3K/AKT pathway is crucial for various cellular functions, including proliferation, migration, inflammation, and permeability. We performed Western blot analysis to explore the potential mechanisms by which PCEVs restored impaired vascular barrier and angiogenic functions; results confirmed that PCEVs improved the levels of Angpt1, p-Tie2, p-PI3K, p-Akt, and p-NF- κ B. In contrast, the Angpt1 siRNA PCEVs group decreased the expression of Angpt1, p-PI3K, and p-Akt and increased the expression of p-NF- κ B (Fig. 6d, Supplemental Fig. 2c). These findings implied that Angpt1 carried by PCEVs promotes the PI3K/Akt pathway while inhibiting the NF- κ B pathway in VECs following LPS stimulation.

PCEV-delivered Angpt1 mediates PC recruitment in mesenteric microvessels after sepsis in vivo

As PCs are crucial for maintaining the vascular endothelial barrier function and can be recruited following PCEV infusion, we used the fluorescent-labeled (PDGFR- β -Cre+ mT/mG) PC transgenic mice to assess the impact of Angpt1 on PCEVs in PC recruitment. The results showed that green fluorescence, which is indicative of PCs, decreased significantly in mesenteric venules and capillaries after sepsis. PCEVs increased PC coverage, while Angpt1 siRNA PCEVs inhibited PC recruitment compared with PCEVs (Fig. 7a). Additionally, electron microscopy revealed that PCs were attached to the EC; however, PC levels decreased after sepsis. While the administration of PCEVs was found to enhance PC recruitment, the use of Angpt1 siRNA PCEV reduced PC recruitment (Fig. 7b). These results show that Angpt1 in PCEV could improve PC recruitment, thereby enhancing vascular barrier function.

PCEV-delivered Angpt1 mediated intestinal barrier function and inflammatory factors after sepsis in vivo

As observed by light microscopy, the sham group had intact intestinal mucosa with neatly arranged intestinal villi. After sepsis, the intestinal mucosa of the septic group showed disintegrated intestinal villi, epithelial cell detachment, and villus tip denudation. Compared to the damage in the septic group, the PCEV treatment group showed reduced intestinal mucosal damage. After low expression of Angpt1 in PCEVs, the Angpt1 siRNA PCEV group showed considerably reduced efficacy compared to the PCEV group (Fig. 8a), and electron microscopy findings of the intestinal villi were consistent with those of HE staining (Fig. 8b). The PCEVs group also showed improved intestinal blood flow; however, the introduction of Angpt1 siRNA PCEVs hindered the beneficial effects of the PCEVs (Fig. 8c). Since the sepsis-induced systemic inflammatory response is closely associated with intestinal damage, serum TNF- α , IL-1 β , and IL-6 were elevated. PCEVs significantly decreased the production of these cytokines, whereas Angpt1 knockout in PCEV increased the production of these cytokines (Fig. 8d). These results suggest that Angpt1 deletion in PCEVs significantly exacerbated sepsis-induced intestinal injury and inflammation.

Discussion

The main findings of this study can be summarized as follows: (1) PCEV administration improved vascular hyperpermeability, intestinal barrier function, PC coverage, and enhanced endothelial proliferation and angiogenic functions after sepsis (Fig. 9); (2) PCEVs expressed a marked amount of Angpt1; and (3) Angpt1 siRNA PCEVs diminished the beneficial effects of PCEVs on vascular barrier function, suggesting that the therapeutic effects of PCEVs are mediated via the Angpt1/PI3K/AKT pathway.

Endothelial dysfunction is a hallmark of acute inflammatory conditions such as sepsis, burns, trauma, and acute respiratory distress syndrome. A key feature of sepsis is enhanced endothelial permeability resulting from the disruption of endothelial adherens and tight junctions, as well as NF- κ B activation [3]. Currently, no

(See figure on next page.)

Fig. 5 Effect of Angpt1 siRNA PCEVs on vascular permeability in septic rats in vivo. **a** Representative microphotographs of the endocytosis of PKH-26-labeled PCEVs in mesenteric venule. Scale bars: 50 μ m. **b** Vascular leakage of mesenteric venules in septic rats (n = 8). Scale bars: 50 μ m. **c** Velocity of red blood cells in mesenteric arterioles and venules (n = 8). **d** Expression of ZO-1 and VE-cadherin in mesenteric venules by western blotting (n = 3). **e** Immunohistochemistry for ZO-1 and VE-cadherin in mesenteric venules. Scale bars: 20 μ m. **f** Representative TEM images of tight junctions in mesenteric venules (red arrows indicate the tight junction; EC, endothelial cell; RBC, red blood cell; TJ, tight junction; L, lumen).

*** $P < 0.01$ vs. Sham, ** $P < 0.01$ vs. Sep, @@ $P < 0.01$ vs. PCEVs (one-way ANOVA)

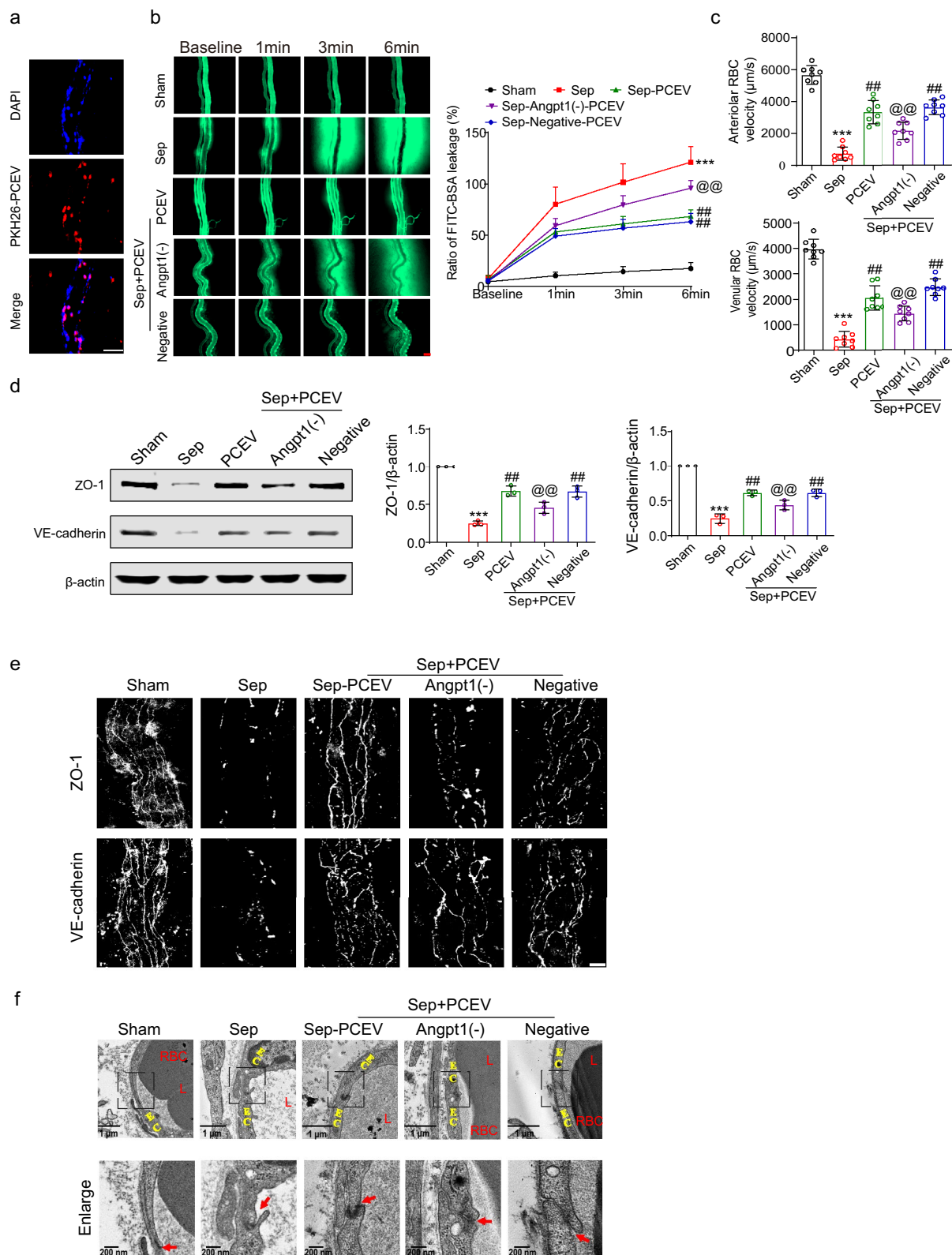


Fig. 5 (See legend on previous page.)

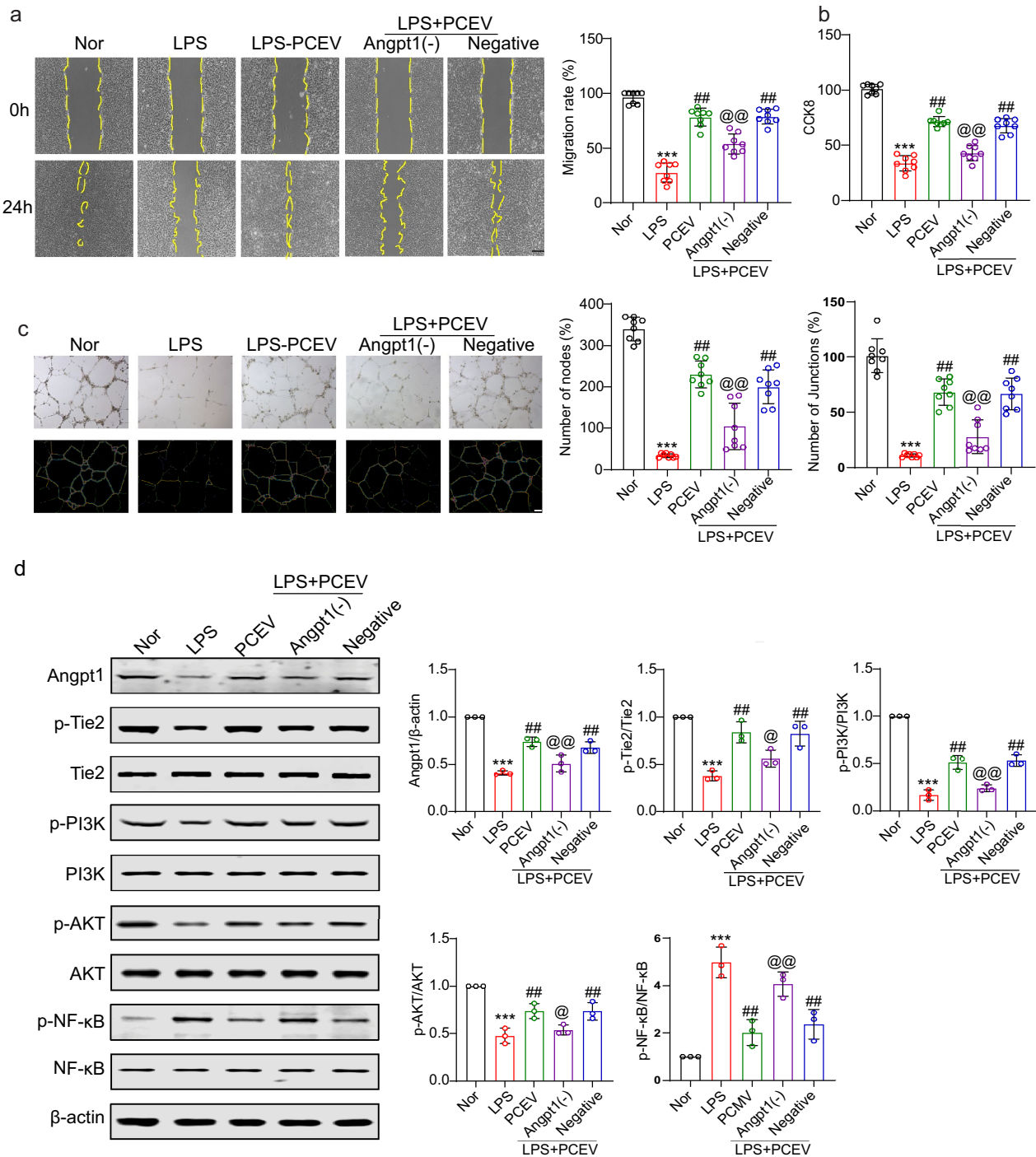


Fig. 6 Angpt1 carried by PCEVs regulates VEC migration, proliferation, and tube formation. **a** Representative microphotographs of the scratch migration assay and the scratched area were shown (n=8). Scale bars: 100 μm. **b** CCK8 proliferation assay of VECs (n=8). **c** Tubular structures were photographed, and the number of nodes and junctions were calculated using the ImageJ software (n=8). Scale bars: 50 μm. **d** Western blot assay was performed to detect Angpt1, p-Tie2, Tie2, p-PI3K, PI3K, p-Akt, Akt, p-NF-κB, NF-κB, and β-actin protein levels (n=3). ****P* < 0.001 vs Nor, ##*P* < 0.01 vs. LPS, @*P* < 0.05, @@*P* < 0.01 vs. PCEV (one-way ANOVA)

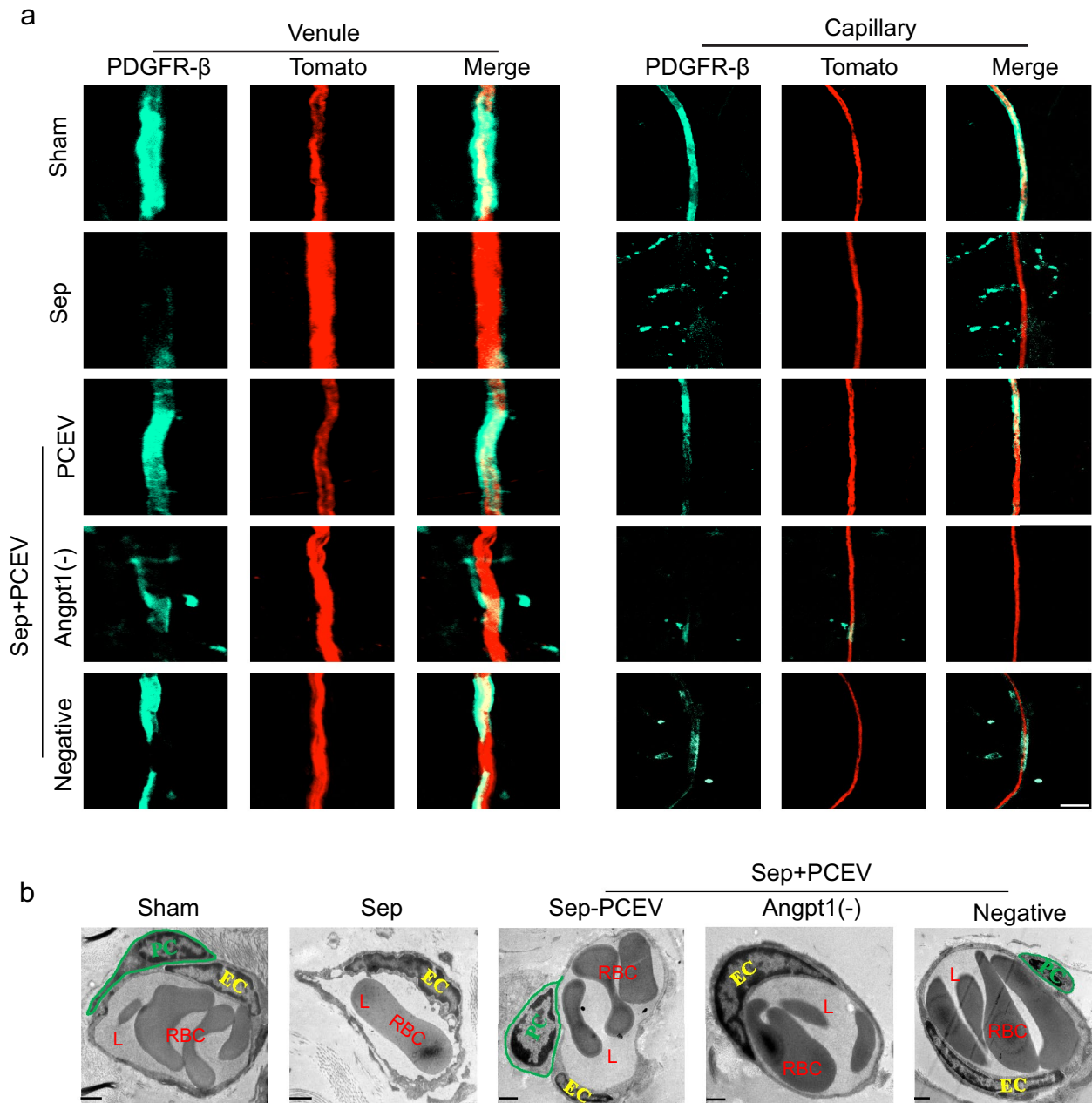


Fig. 7 Effect of Angpt1 siRNA PCEVs on vascular PC coverage after sepsis in vivo. **a** In vivo image of the mesenteric venules and capillaries of PDGFR-β-Cre + mT/mG transgenic mice showing green-expressing pericytes (PCs) on mesenteric microvessels with Tomato (red) expression in all membranes after sepsis. Scale bars: 20 μm. **b** Representative TEM images of PCs in mesenteric venules in septic rats (green indicates PC; EC, endothelial cell; RBC, red blood cell; L, lumen). Scale bars: 1 μm

targeted medications are available for treating microvascular damage; however, given the significant impact of endothelial breakdown and microcirculatory dysfunction following sepsis, developing effective strategies to protect the endothelium is important. The findings of this study showed that PCEVs increased the expression of ZO-1 and VE-cadherin, restored microvascular blood flow,

and decreased NF-κB activation and pro-inflammatory cytokines such as TNF-α, IL-6, and IL-1β.

PCs are components of stem cell niches and mesenchymal stem cells located between the ECs of capillaries and the basement membrane. Stem cells play an important role in the treatment of sepsis; for example, MSC-EV therapy inhibits pathogen replication and activates

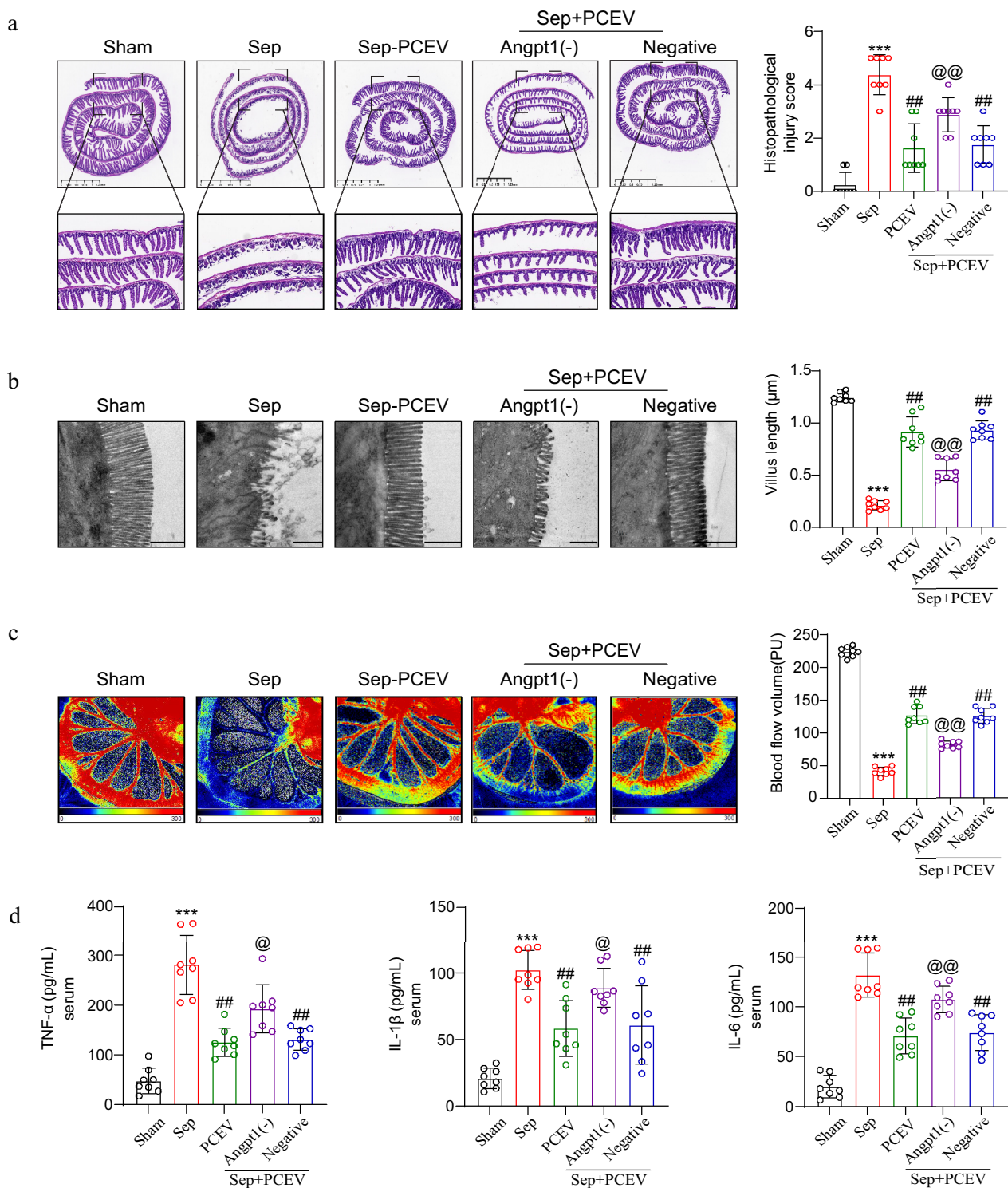


Fig. 8 Effect of Angpt1 siRNA PCEVs on intestinal barrier function and inflammatory factors post-sepsis in vivo. **a** Representative images of HE-stained sections of Swiss roll mounts of the entire small intestine, evaluated based on the histologic injury scores (n=8). **b** TEM images of villus structural morphology, small intestinal, and villus lengths were measured (n=8). Scale bars: 1 μm. **c** Blood flow in the intestine evaluated by laser speckle imaging (n=8). **d** Blood levels of TNF-α, IL-1β, and IL-6 were measured by ELISA after sepsis (n=8). ***P < 0.01 vs. Sham, ##P < 0.01 vs. Sep, @P < 0.05 and @@P < 0.01 vs. PCEVs (one-way ANOVA)

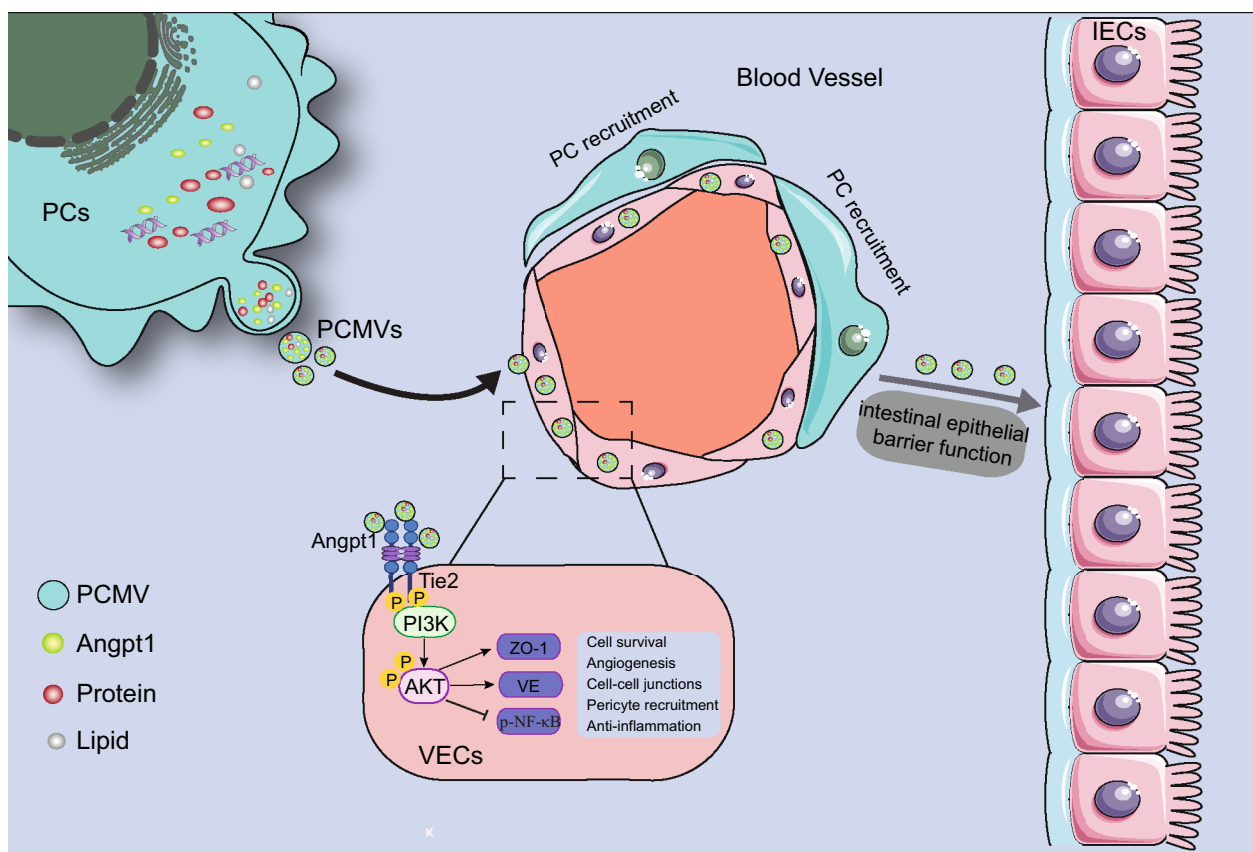


Fig. 9 Schematic of the mechanism of the therapeutic effect of PCEVs on gut barrier function post-sepsis. PCEVs delivered Angpt1 to VECs, synergistically improving the cell junctions, angiogenesis, anti-inflammation, and PC recruitment by activating the p-PI3K/AKT pathway, thereby enhancing vascular endothelial barrier function. Furthermore, the intestinal epithelial barrier function was also restored

phagocytic function and anti-inflammatory activity [21]. However, limited information is available on PCEVs. The experiments in this study found that PCEVs contain growth factors with the most enriched factor being Angpt1. Angpt1 is a critical endothelial survival and vascular stabilizing factor, and the axis of the endothelial receptor Angpt1/Tie2 plays an essential role in restoring vascular barrier function [12] by activating the PI3K/Akt signaling pathway, reducing inflammation, and improving cell junctions. We also found that PCEVs improved the expression of p-Tie2, p-PI3K, and p-AKT; as this effect was eliminated by Angpt1 siRNA PCEVs, an essential role of Angpt1 in PCEVs for restoring vascular barrier function was suggested.

This study has some limitations. First, recent studies have shown that EVs released by PCs contain various angiogenic factors, such as Angpt1, VEGF, and CTGF, which exhibit beneficial effects [22, 28]. Our previous study showed that CTGF contained in PCEVs ameliorated vascular endothelial damage after sepsis [9]. This research revealed that Angpt1 in PCEVs also had a protective effect on vascular endothelial cells. Interference

with Angpt1 markedly diminished the protective efficacy of PCEVs, but some degree of protective action remained, suggesting that CTGF carried by PCEVs may contribute to the protective effect. Building upon prior research, we hypothesized that Angpt1 and CTGF carried by PCEVs may play a synergistic role in protecting vascular endothelial function after sepsis, which requires further verification.

Secondly, we found that PCEVs enhanced PC recruitment and improved intestinal barrier function. The mechanisms governing PC migration and recruitment are complex and have not yet been fully established. However, current literature suggests that Angpt1/Tie, PDGF/PDGFR- β , S1P/EDG-1, PI3K/AKT, TGF- β , Notch1, and MMP activity regulate the recruitment of PCs [21]. Therefore, the exact molecular mechanisms, particularly regarding Angpt1's role in PC recruitment and microvascular regulation, remain unclear and warrant further investigation. Additionally, the involvement of ECs, PCs, and enteric glial cells in the gut-vascular barrier (GVB) has received significant focus as an additional factor for the regulation of the

intestinal barrier [22]. Some studies have shown that GVB was restored in a model of diabetes and may improve the gut epithelial barrier [28, 21]. In this study, we found that PCEVs could improve VEC functions, PC coverage, and intestinal barrier function, suggesting that PCEV has the ability to restore GVB to improve the integrity of the gut epithelium. Other studies showed that mesenchymal stem cell-derived EVs could directly protect intestinal epithelial barrier function by activating the PI3K/Akt signaling pathway after inflammatory bowel disease [22, 28]. In this study, PCEV was administered intravenously, raising the question of whether PCEV directly affects intestinal barrier function or whether the improvement is mediated by enhancing the microvascular environment.

Recent studies have suggested that PCs play a crucial role in the mechanism of immune function regulation and thus may be a therapeutic target in disorders as diverse as stroke, traumatic brain injury, migraine, epilepsy, and spinal cord injury [21]. PCs could be targeted to develop novel therapeutic approaches to neurological disorders by regulating immune cell entry to the central nervous system [22]. Lastly, although the protective effects of PCEVs were demonstrated, their potential immunomodulatory effects in sepsis and other inflammatory conditions require more comprehensive analyses to determine their broader therapeutic utility.

Conclusion

In summary, EVs released from PCs exerted protective effects on the vascular endothelial and intestinal epithelial barrier functions in a rat model of CLP-induced sepsis. More importantly, the underlying mechanism of the action of PCEVs may be mediated via the Angpt1/PI3K/AKT pathway. Thus, sepsis-induced vascular hyperpermeability plays a causative role in vascular dysfunction, making PCEVs a promising therapeutic target in these pathologies.

Abbreviations

PC	Pericyte
EVs	Extracellular vesicles
TEM	Transmission electron microscopy
EC	Endothelial cell
PCEV	Extracellular vesicles derived from pericytes
SEV	Smooth muscle cell-derived extracellular vesicle
CLP	Cecal ligation and puncture
FITC-BSA	Fluorescein isothiocyanate-bovine serum albumin
TER	Transendothelial electrical resistance
VECs	Vascular endothelial cells
VSMCs	Vascular smooth muscle cells
MODS	Multi-organ dysfunction syndrome
Angpt1	Angiotensinogen-converting enzyme 1
VEGF	Vascular endothelial growth factor
TGF- β	Transforming growth factor- β

GO	Gene ontology
SD	Sprague–Dawley
GVB	Gut-vascular barrier
RMP	Retinal microvascular pericytes
PBS	Phosphate-buffered saline
MOI	Multiplicity of infection
ELISA	Enzyme-linked immunosorbent assay
RT	Room temperature
DEGs	Differentially expressed genes

Supplementary Information

The online version contains supplementary material available at <https://doi.org/10.1186/s13287-025-04201-z>.

Supplementary file 1.
Supplementary file 2.
Supplementary file 3.
Supplementary file 4.
Supplementary file 5.
Supplementary file 6.
Supplementary file 7.
Supplementary file 8.
Supplementary file 9.

Acknowledgements

We thank the Instrumental Analysis Center of Army Medical University for the assistance in material characterizations.

Author contributions

ZSZ, AY, and XL contributed equally to this work. ZSZ, AY, and XL performed the experiments, collected data, and prepared the manuscript. YYL, DQB, JZ, JTZ, and QHL participated in the animal study and data analysis. HNZ contributed to the proteomic analysis. TL and LML conceived the study, participated in design and coordination, and edited the manuscript. All authors read and approved the final version of the manuscript. The authors declare that they have not used AI-generated work in this manuscript.

Funding

This study was supported by the Young Scientists Fund (82102279), the Key Projects of the National Natural Science Foundation of China (82330079), and the Science Foundation of State Key Laboratory of Trauma and Chemical Poisoning (2024K003).

Availability of data and materials

All data generated or analyzed during this study are included in this published article.

Declarations

Ethics approval and consent to participate

This study received approval from the Laboratory Animal Welfare and Ethics Committee of Third Military (Army) Medical University (Title of the approved project: Glycolysis enhances the efficacy of pericyte transendothelial migration on vascular leakage after septic shock by lactylation of fascin and its mechanism; Approval number: AMUWEC20210873; Date of approval: 05/03/2021). All animal experiments were conducted under university guidelines.

Consent for publication

Not applicable.

Competing interests

The authors declare that they have no competing interests.

Author details

¹State Key Laboratory of Trauma, Burns and Combined Injury, Department of Shock and Transfusion, Daping Hospital, Army Medical University, Chongqing 400042, China. ²Department of Anesthesiology, Daping Hospital, Army Medical University, Chongqing 400042, China.

Received: 30 August 2024 Accepted: 29 January 2025

Published online: 12 February 2025

References

- Gyawali B, Ramakrishna K, Dharamoon AS. Sepsis: the evolution in definition, pathophysiology, and management. *SAGE Open Med.* 2019;7:2050312119835043.
- Tang F, Zhao XL, Xu LY, Zhang JN, Ao H, Peng C. Endothelial dysfunction: pathophysiology and therapeutic targets for sepsis-induced multiple organ dysfunction syndrome. *Biomed Pharmacother.* 2024;178: 117180.
- McMullan RR, McAuley DF, O'Kane CM, Silversides JA. Vascular leak in sepsis: physiological basis and potential therapeutic advances. *Crit Care.* 2024;28(1):97.
- Zhang ZS, Zhou HN, He SS, Xue MY, Li T, Liu LM. Research advances in pericyte function and their roles in diseases. *Chin J Traumatol.* 2020;23(2):89–95.
- Su H, Cantrell AC, Zeng H, Zhu SH, Chen JX. Emerging role of pericytes and their secretome in the heart. *Cells.* 2021;10(3):548.
- Dave KM, Venna VR, Rao KS, Stolz DB, Brady B, Quaicoe VA, et al. Mitochondria-containing extracellular vesicles from mouse vs. human brain endothelial cells for ischemic stroke therapy. *J Control Release.* 2024;373:803–22.
- Welsh JA, Goberdhan DCI, O'driscoll L, Buzas EI, Blenkinsop C, Bus-solati B, et al. Minimal information for studies of extracellular vesicles (MISEV2023): From basic to advanced approaches. *J Extracell Vesicles.* 2024;13(2):e12404.
- Zhang ZS, Liu YY, He SS, Bao DQ, Wang HC, Zhang J, et al. Pericytes protect rats and mice from sepsis-induced injuries by maintaining vascular reactivity and barrier function: implication of miRNAs and microvesicles. *Mil Med Res.* 2023;10(1):13.
- Zhou H, Zheng D, Wang H, Wu Y, Peng X, Li Q, et al. The protective effects of pericyte-derived microvesicles on vascular endothelial functions via CTGF delivery in sepsis. *Cell Commun Signal.* 2021;19(1):115.
- Kato K, Dieguez-Hurtado R, Park DY, Hong SP, Kato-Azuma S, Adams S, et al. Pulmonary pericytes regulate lung morphogenesis. *Nat Commun.* 2018;9(1):2448.
- Uemura MT, Maki T, Ihara M, Lee VMY, Trojanowski JQ. Brain microvascular pericytes in vascular cognitive impairment and dementia. *Front Aging Neurosci.* 2020;12:80.
- David S, Kumpers P, Van Slyke P, Parikh SM. Mending leaky blood vessels: the angiotensin-Tie₂ pathway in sepsis. *J Pharmacol Exp Ther.* 2013;345(1):2–6.
- Li G, Gao J, Ding P, Gao Y. The role of endothelial cell-pericyte interactions in vascularization and diseases. *J Adv Res.* 2025;67:269–288.
- Hayakawa K, Esposito E, Wang X, Terasaki Y, Liu Y, Xing C, et al. Transfer of mitochondria from astrocytes to neurons after stroke. *Nature.* 2016;535(7613):551–5.
- Moolenbeek C, Ruitenber EJ. The "Swiss roll": a simple technique for histological studies of the rodent intestine. *Lab Anim.* 1981;15(1):57–9.
- Ji AL, Li T, Zu G, Feng DC, Li Y, Wang GZ, et al. Ubiquitin-specific protease 22 enhances intestinal cell proliferation and tissue regeneration after intestinal ischemia reperfusion injury. *World J Gastroenterol.* 2019;25(7):824–36.
- Zhang SS, Hu JQ, Liu XH, Chen LX, Chen H, Guo XH, et al. Role of moesin phosphorylation in retinal pericyte migration and detachment induced by advanced glycation endproducts. *Front Endocrinol (Lausanne).* 2020;11: 603450.
- Gaceb A, Ozen I, Padel T, Barbariga M, Paul G. Pericytes secrete pro-regenerative molecules in response to platelet-derived growth factor-BB. *J Cereb Blood Flow Metab.* 2018;38(1):45–57.
- Scarff CA, Fuller MJG, Thompson RF, Iadanza MG. Variations on negative stain electron microscopy methods: tools for tackling challenging systems. *J Vis Exp.* 2018;(132):57199.
- Deleu S, Arnauts K, Deprez L, Machiels K, Ferrante M, Huys GRB, Thevelein JM, Raes J, Vermeire S. High acetate concentration protects intestinal barrier and exerts anti-inflammatory effects in organoid-derived epithelial monolayer cultures from patients with ulcerative colitis. *Int J Molecular Sci.* 2023;24(1):768.
- Cox J, Mann M. MaxQuant enables high peptide identification rates, individualized p.p.b.-range mass accuracies and proteome-wide protein quantification. *Nat Biotechnol.* 2008;26(12):1367–72.
- Arnaoutova I, Kleinman HK. In vitro angiogenesis: endothelial cell tube formation on gelled basement membrane extract. *Nat Protoc.* 2010;5(4):628–35.
- You J, Fu Z, Zou L. Mechanism and potential of extracellular vesicles derived from mesenchymal stem cells for the treatment of infectious diseases. *Front Microbiol.* 2021;12: 761338.
- Van Hulle C, Ince S, Okonkwo OC, Bendlin BB, Johnson SC, Carlsson CM, et al. Elevated CSF angiotensin-2 correlates with blood-brain barrier leakiness and markers of neuronal injury in early Alzheimer's disease. *Transl Psychiatry.* 2024;14(1):3.
- Sharma K, Zhang Y, Paudel KR, Kachelmeier A, Hansbro PM, Shi X. The emerging role of pericyte-derived extracellular vesicles in vascular and neurological health. *Cells.* 2022;11(19):3108.
- Yang HL, Thiyagarajan V, Shen PC, Mathew DC, Lin KY, Liao JW, et al. Anti-EMT properties of CoQ0 attributed to PI3K/AKT/NFKB/MMP-9 signaling pathway through ROS-mediated apoptosis. *J Exp Clin Cancer Res.* 2019;38(1):186.
- Di Tommaso N, Santopaolo F, Gasbarrini A, Ponziani FR. The gut-vascular barrier as a new protagonist in intestinal and extraintestinal diseases. *Int J Mol Sci.* 2023;24(2):1470.
- Barry M, Trivedi A, Pathipati P, Miyazawa BY, Vivona LR, Togarrati PP, et al. Mesenchymal stem cell extracellular vesicles mitigate vascular permeability and injury in the small intestine and lung in a mouse model of hemorrhagic shock and trauma. *J Trauma Acute Care Surg.* 2022;92(3):489–98.
- Duan Y, Prasad R, Feng D, Beli E, Li Calzi S, Longhini ALF, et al. Bone marrow-derived cells restore functional integrity of the gut epithelial and vascular barriers in a model of diabetes and ACE2 deficiency. *Circ Res.* 2019;125(11):969–88.
- Duan L, Huang H, Zhao X, Zhou M, Chen S, Wang C, et al. Extracellular vesicles derived from human placental mesenchymal stem cells alleviate experimental colitis in mice by inhibiting inflammation and oxidative stress. *Int J Mol Med.* 2020;46(4):1551–61.
- Chen J, Luo Y, Li Y, Chen D, Yu B, He J. Chlorogenic acid attenuates oxidative stress-induced intestinal epithelium injury by co-regulating the PI3K/Akt and IkappaBalpha/NF-kappaB signaling. *Antioxidants (Basel).* 2021;10(12):1915.
- Török O, Schreiner B, Schaffnerath J, Tsai H-C, Maheshwari U, Stifter SA, et al. Pericytes regulate vascular immune homeostasis in the CNS. *Proc Natl Acad Sci USA.* 2021;118(10):e2016587118.
- Cheng J, Korte N, Nortley R, Sethi H, Tang Y, Attwell D. Targeting pericytes for therapeutic approaches to neurological disorders. *Acta Neuropathol.* 2018;136(4):507–23.

Publisher's Note

Springer Nature remains neutral with regard to jurisdictional claims in published maps and institutional affiliations.